

Rapid evaluation and quantitative analysis of eugenol derivatives in essential oils and cosmetic formulations on human skin using attenuated total reflectance–infrared spectroscopy

Lai-Hao Wang* and Wei-Chien Sung

Department of Medical Chemistry, Chia Nan University of Pharmacy and Science, Tainan, Taiwan

Abstract. We studied the fragrances 4-allylbenzenes (eugenol, methyl eugenol, acetyl eugenol) as well as 4-propenylbenzenes (isoeugenol) in commercial essential oils using a fast and nondestructive attenuated total reflectance–infrared (ATR–IR) spectroscopy method. The method was based on ATR–IR utilizing partial least square regression. The calibrations were modeled in the characteristic *region* for eugenol (1430–1432 cm^{-1}), isoeugenol (960–970 cm^{-1}) and methyl eugenol (803–807 cm^{-1}). The models were then applied to predict the percutaneous absorption process yield and to monitor the concentrations of eugenol derivatives on human skin.

Keywords: Eugenol derivatives, essential oils and cosmetic formulations, ATR–IR

1. Introduction

The structurally related substituted p-allylbenzenes derivatives eugenol, methyl eugenol and acetyl eugenol occur naturally in a variety of traditional foods, particularly in spices such as cloves, cinnamon and basil [20]. Volatile compounds of clove oil, which is usually used as a flavoring, and the main chemical components of clove oil are eugenol, acetyl eugenol, isoeugenol and caryophyllene [1,11,21]. It has been demonstrated to be an effective, inexpensive anesthetic agent, antioxidant and blood circulation enhancer [6,7,9]. Commercially available essential oils have been analyzed using gas chromatography (GC) and gas chromatography–mass spectrometry (GC–MS), and the main ingredients of each essential oil have been quantified [12]. GC/MS analyses of p-allylbenzenes such as asarone and methyl eugenol have also been done [5,15,19]. Mass spectroscopy is not entirely satisfactory for isomers such as eugenol and isoeugenol, which have the same mass spectral data (m/z). The literature reports that infrared (IR) spectroscopy provides accurate information on molecular vibration in a short time, and that it has been used to analytically characterize essential oils in recent years [2–4,16–18]. There are

*Corresponding author: Lai-Hao Wang, Department of Medical Chemistry, Chia Nan University of Pharmacy and Science, 60 Erh-Jen Road, Section 1, Jen Te, Tainan 71743, Taiwan. E-mail: e201466.wang@msa.hinet.net.

a number of studies [8,10,13] that use attenuated total reflection (ATR) combined with IR to quantitatively detect ingredients in foods and plant oils, which makes handling liquid samples more convenient and analyzing essential oils more rapid. The zinc selenide flattop plate is suitable for skin, films and polymers. However, to our knowledge, the percutaneous absorption of only a few eugenol derivatives in essential oil emulsions has been investigated. We previously developed an isocratic reversed phase liquid chromatography with fluorometric detection and gas chromatography methods to measure the concentration of eugenol in human serum [23,24]. Because these techniques are generally time-consuming and expensive, they are not well-suited for routine analysis. Furthermore, analysis of the surface absorption of chemicals on the skin is affected by the choice of ATR crystal. Human skin is usually the preferred skin membrane to use in an absorption study: no animal model gives absorption values identical to those obtained in human skin. GC/MS analysis shows that the main constituents of essential oils are terpenes and terpenoids. Terpenoid compounds are percutaneous permeation enhancers; they are believed to act by disrupting the ordered lipid structure of the stratum corneum and by increasing partitioning of the drug from the aqueous vehicle into the stratum corneum [14]. We previously [22] evaluate the contribution of ATR-FTIR spectroscopy plus fluorescence detection as an *in vivo* analytical tool for determining the percutaneous penetration of p-aminobenzoic acid and measuring its metabolites in human urine. The aim of the present study was to create a method for rapid screening of eugenol derivatives in commercial essential oils and construct a linear calibration model to determine eugenol derivatives in human skin after treatment with various formulations.

2. Experimental section

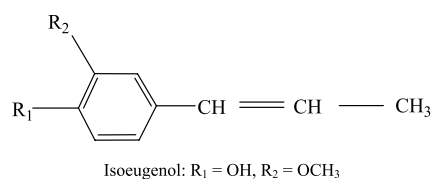
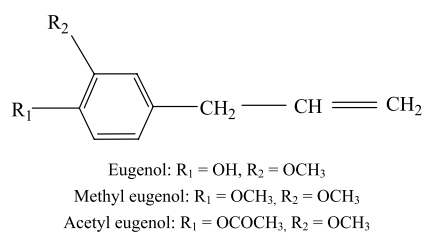
2.1. Apparatus and materials

The absorption spectra of essential oils and human skin were determined using a spectrophotometer (2000/IRDM FTIR; Perkin-Elmer, Fremont, CA, USA) with an ATR system (Gateway ATR; Specac Inc., Smyrna, GA (now Cranston, RI), USA). An ATR crystal material should be chosen by the sample's useful pH range. For zinc selenide, the most common internal reflection element (IRE), a pH between 5 and 9 is required ($n = 2.4$). Approximately 50 μl of the essential oils were placed on the surface of the ZnSe-ATR crystal. Because of the high signal-to-noise ratio on this instrument, 10 scans (in the range of 4000–400 cm^{-1}) at 4 cm^{-1} resolution were sufficient to obtain spectra adequate for quantitation. All other reagents were of analytical grade.

2.2. Sample materials and target fragrance substances

The essential oils that we investigated were purchased at a local department store. They were labeled as 100% natural products (*Myristica fragrans*: nutmeg 1 and 2, *Cinnamomum cassia*: cassia bark, *Cinnamomum zeylanicum*: cinnamon, *Foeniculum vulgare*: fennel 1, *Foeniculum dulce*: fennel 2, *Thymus vulgaris* thyme 1 and 2, *Pimpinella anisum*: aniseed, *Eugenia caryophyllata*: clove). Some oils had different lot numbers but the same manufacturer, and some had different lot numbers and different manufacturers.

Pure standard substances (the target fragrance substances) were purchased elsewhere: eugenol and isoeugenol (Acros Organics, Geel, Belgium); methyl eugenol and acetyl eugenol (TCI, Tokyo Chemical Industry Co., Ltd., Tokyo, Japan). The chemical structures of the fragrances and related substituted allylbenzene derivatives are shown in Scheme 1.



Scheme 1. The fragrance structures of eugenol and its derivatives.

2.3. Formulations

Test materials. There were three different eugenol-derivative application vehicles: (A) water-in-oil (w/o), (B) oil-in-water (o/w) and (C) nano-emulsions (nano) included in this study. We used a hydrophobic emulsion containing (A) jojoba oil 20% (w/w), tricaprylin 20% (w/w), Tween 80 10% (w/w), Span 40 10% (w/w) and distilled 40% in w/o emulsion; a hydrophilic emulsion containing (B) stearic (octadecanoic) acid 1.7% (w/w), Tween 80 10% (w/w), Span 40 10% (w/w) and distilled 78% in o/w emulsion; and a nano-emulsion (C) lauric (dodecanoic) acid 0.8% (w/w), AOT [sodium bis(2-ethylhexyl) sulfosuccinate] 8% (w/w) and distilled 92%.

2.4. Constructing the calibration model of eugenol derivatives in the vehicles

To calibrate the absorbance of eugenol derivatives in an emulsion, the emulsion samples (100 μl) were applied with a pipette and distributed homogeneously with a spatula over an area of $7 \times 2 \text{ cm}^2$ on human skin for FTIR measurements. The marked skin area of the palm was pressed on the ZnSe crystal (the window of the Skin Analyzer) using its own weight. After each measurement, the window was cleaned with alcohol. All *in vivo* spectra were obtained under ambient laboratory conditions and recorded at $t = 0$ (before applying the emulsion) and at $t = 30$ and 60 min after applying the emulsion. At each time, the values of the absorption band integrations were evaluated for their characteristic frequencies: 1430–1432, 960–970 and 803–807 cm^{-1} for eugenol, isoeugenol and methyl eugenol, respectively.

3. Results and discussion

3.1. Interpretation of eugenol derivatives spectra

Detailed spectral analysis of the investigated fragrances is based on their vibrational spectra. The IR region between 1700 and 700 cm^{-1} is characteristic of the fingerprint region that provides complex but unique and reproducible spectral information with a significant contribution for substance identification. All of these fragrances show some characteristic frequencies that can be used for differentiating among

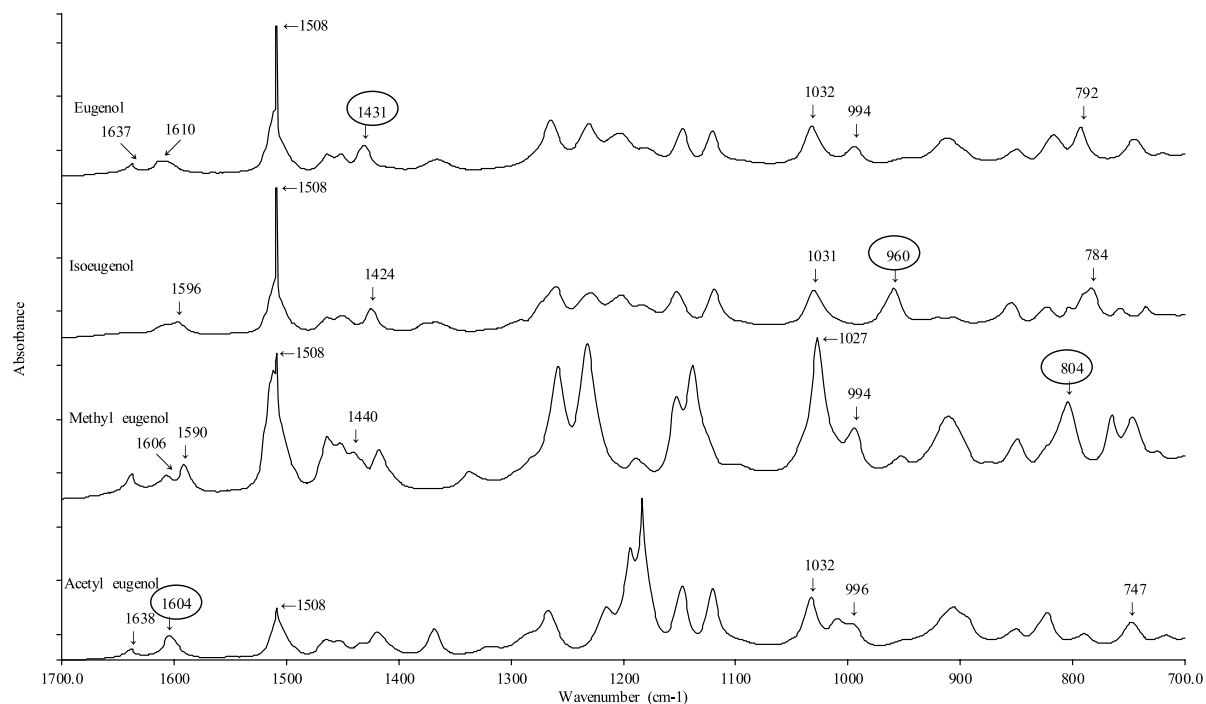


Fig. 1. Eugenol, isoeugenol, methyl eugenol and acetyl eugenol spectra obtained using attenuated total reflectance–infrared Fourier transform spectroscopy (ATR–IR).

them. The ATR–IR of the eugenol derivatives were recorded (Fig. 1). As can be seen in Fig. 1, the spectral signal obtained at the frequencies of 1431, 960, 804 and 1604 cm^{-1} can be attributed to the presence of CH_2 deformation vibration, trans CH out-of-plane, ring deformation, and the $\text{C}=\text{C}$ aromatic band in ATR–IR for eugenol, isoeugenol, methyl eugenol and acetyl eugenol, respectively. Isometric compounds like eugenol and isoeugenol show significant differences in ATR–IR. Spectral CH out-of-plane of eugenol is seen at 994 cm^{-1} , while for isoeugenol this corresponding signal appears at 960 cm^{-1} (Fig. 1). Eugenol derivatives have the same intensive peak at 1027–1032 cm^{-1} in IR. These bands can be attributed to trans CH in phase wag.

To identify the components of commercial essential oils, four components of commercial fragrances were analyzed by comparing the characteristic frequencies and comparing them with those of authentic standards (Table 1).

3.2. Sensitivity

The ATR–IR absorbance measurements of (A) nutmeg essential oil placed directly onto the ZnSe crystal and of (B) human palm skin treated with nutmeg essential oil are shown in Fig. 2. There are prominent spectral features of nutmeg essential oil at 1431 cm^{-1} (strong absorption band), 960 cm^{-1} (medium strong absorption band) and 804 cm^{-1} (strong absorption band), but at 1604 cm^{-1} it is very weak in ATR for eugenol, isoeugenol, methyl eugenol and acetyl eugenol, respectively. Therefore, these strong absorption bands were chosen to create an absorption plot. In order to quantify the amount of adsorbed eugenol derivatives, a calibration was needed. To calibrate absorbance measurements, an area

Table 1
Essential oils absorbances (peak area) observed infrared (ATR-FTIR) spectra

Essential oils	Characteristic frequencies		
	Eugenol 1430–1432 (cm^{-1})	Isoeugenol 960–970 (cm^{-1})	Methyl eugenol 803–807 (cm^{-1})
Clove	1.6986	– ^a	–
Cassia bark	–	2.8554	–
Cinnamon	–	2.2155	–
Thyme white	–	1.323	–
Thyme	–	1.0463	–
Aniseed	–	0.9029	–
Fennel 1	–	1.5504	–
Fennel 2	–	1.6213	–
Nutmeg 1	0.2389	0.0249	0.0705
Nutmeg 2	0.2031	0.0218	0.0888

^a Not determined.

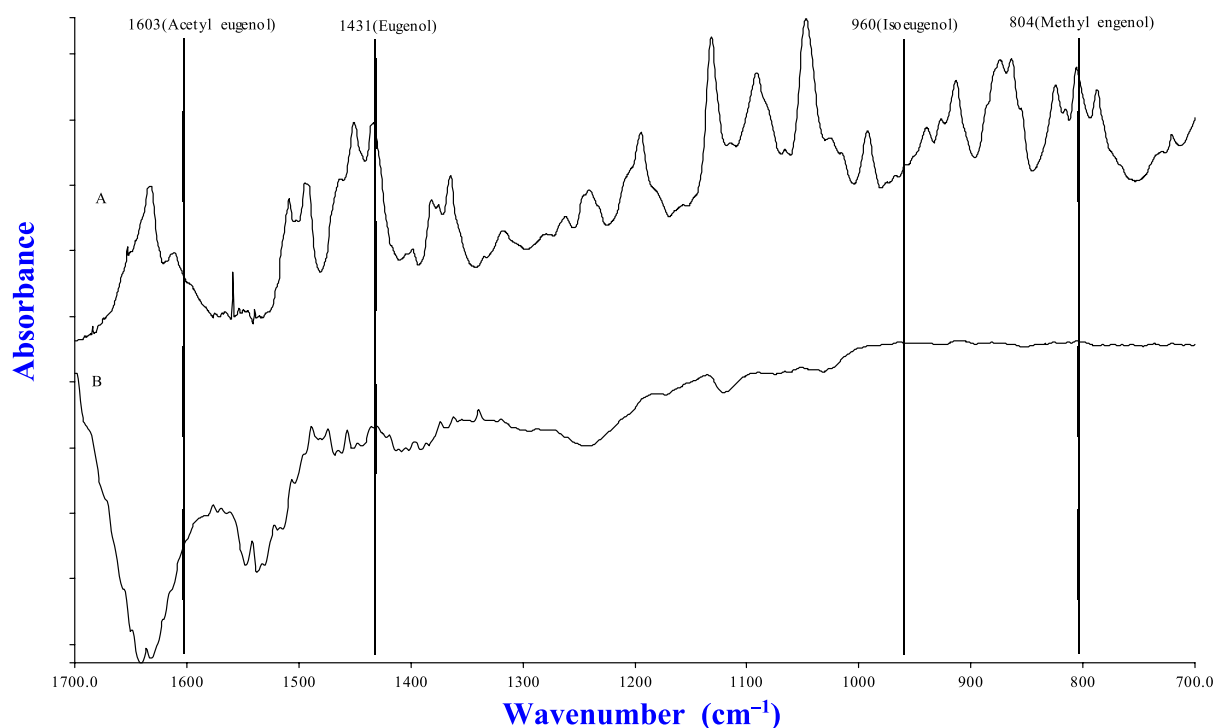


Fig. 2. ATR-IR spectra of (A) nutmeg essential oil direct placed onto a zinc-selenium (ZnSe) crystal and of (B) human palm skin treated with nutmeg essential oil. (Colors are visible in the online version of the article; <http://dx.doi.org/10.3233/SPE-2011-0526>.)

of $7 \times 2 \text{ cm}^2$ was marked on the palm. A 100- μl aliquot of a solution of eugenol derivatives of known concentration in emulsion was spread on the marked area. An effort was made to keep the distribution of the emulsion uniform over the 14 cm^2 area. The absorbance bands of CH_2 at 1431 cm^{-1} and CH at

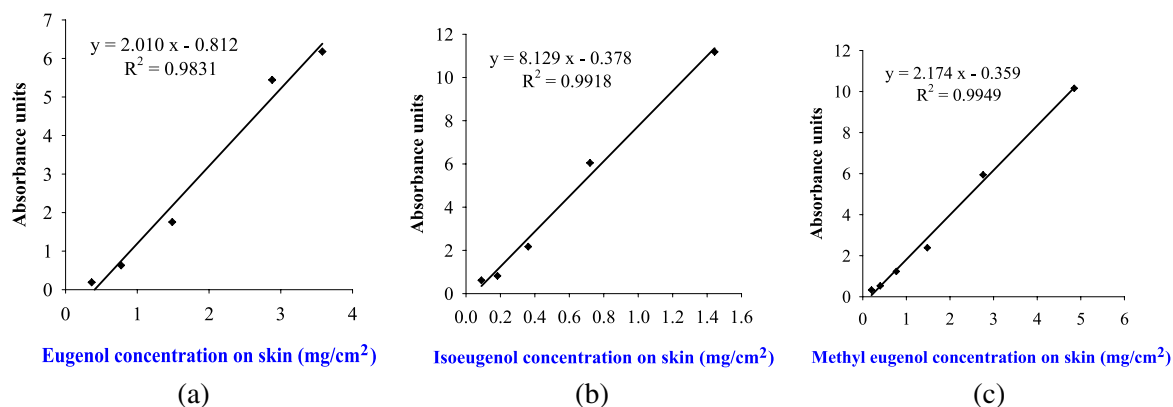


Fig. 3. The linearity of absorbance versus the weight of (a) eugenol, (b) isoeugenol and (c) methyl eugenol in human skin treated with emulsion. (Colors are visible in the online version of the article; <http://dx.doi.org/10.3233/SPE-2011-0526>.)

960 cm^{-1} , and the ring deformation at 804 cm^{-1} were observed using ATR-FTIR spectra on human skin after it had been treated with commercial essential oils containing eugenol derivatives; the results were plotted versus the mg/cm^2 of the standard essential oils applied to the skin. Calibration models for determining eugenol derivatives in emulsion and the ATR-IR estimated concentrations (Fig. 3) showed correlation coefficients > 0.98 . The sensitivity of the instrument can be assessed by looking at the slope of concentration versus the peak area, which is largest for the eugenol derivatives on the ZnSe crystal. Next, eugenol derivatives with slopes of 2.010 (absorbance units to mg/cm^2), 8.129 and 2.174 were obtained for eugenol, isoeugenol and methyl eugenol, respectively.

3.3. Application to human skin (percutaneous absorption of eugenol derivatives)

In this experiment, we evaluated the amount of eugenol derivatives percutaneously absorbed by measuring the amount of eugenol derivatives that remained on the skin surface. The infrared absorbance spectra of human skin with essential oil (a) after (b, c and d) treatment with a substance containing essential oil in w/o, o/w, and nano-emulsions (Figs 4–6) show that the bands at 970, 805 and 1431 cm^{-1} correspond to trans CH out-of-plane, ring deformation, and CH_2 deformation vibration, respectively. From Table 2 and Fig. 7, nano-emulsion as a vehicle showed that the concentrations of eugenol derivatives apparently decreased with time 41.9, 14.7 and 10.4 (mg/cm^2); 87.7, 38.5 and 24.2 (mg/cm^2); and 25.4, 18.4, and 16.3; for eugenol, isoeugenol and methyl eugenol at 0, 30 and 60 min, respectively. Figure 8 shows the isoeugenol concentration-time profiles for human skin after it had been treated with essential oil in a w/o micro-emulsion, o/w-emulsion and nano-emulsion; concentrations clearly decreased over time, but the decrease in the concentration of methyl eugenol was not time-dependent in the w/o emulsion (Fig. 8(a)). It is possible to conclude that the nano-emulsion formulation is an efficacious carrier for the transdermal delivery of isoeugenol.

4. Conclusion

Attenuated total reflectance-infrared (ATR-IR) spectroscopy was used to rapidly screen eugenol derivatives in commercial essential oils. The characteristic frequencies of the bands for fragrances (Fig. 1) were used as the basis for quantitating eugenol derivatives on human skin. ATR-IR spectroscopy

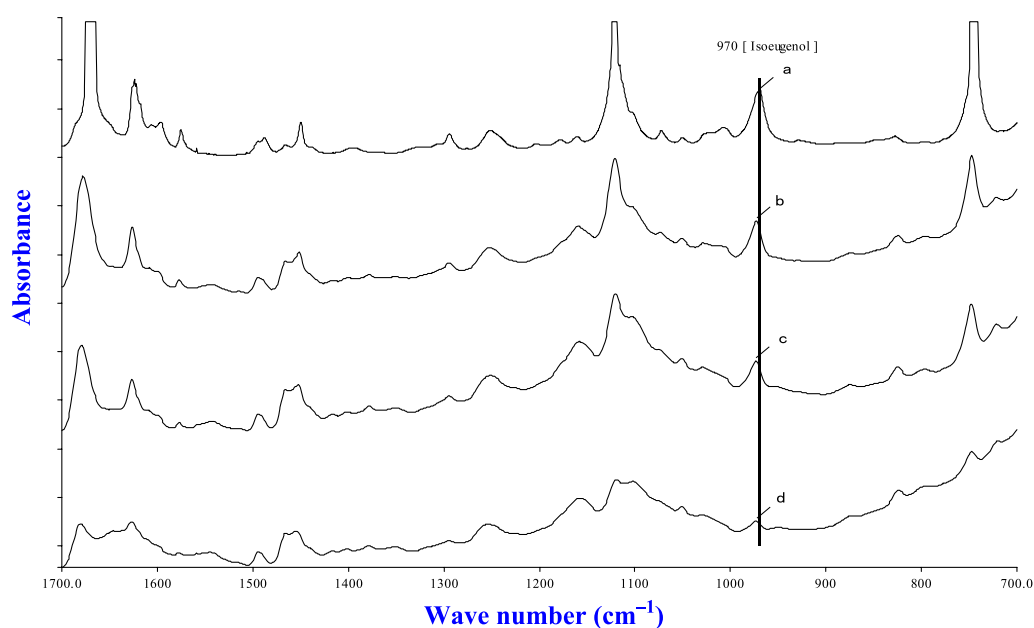


Fig. 4. ATR-IR spectra of human palm skin treated with (a) cassia bark essential oil without w/o emulsion; (b) cassia bark essential oil in w/o emulsion at 0 min; (c) cassia bark essential oil in w/o emulsion at 30 min; (d) cassia bark essential oil in w/o emulsion at 60 min; for the trans CH out-of-plane (characteristic) (970 cm^{-1}). (Colors are visible in the online version of the article; <http://dx.doi.org/10.3233/SPE-2011-0526>.)

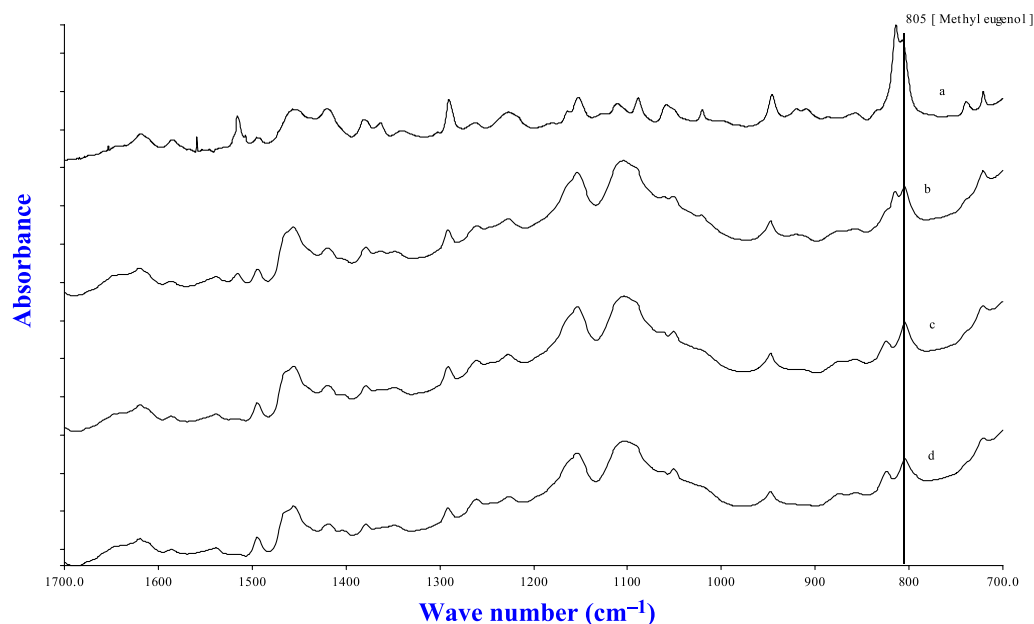


Fig. 5. ATR-IR spectra of human palm skin treated with (a) thyme white essential oil without o/w emulsion; (b) thyme white essential oil in w/o emulsion at 0 min; (c) thyme white essential oil in w/o emulsion at 15 min; (d) thyme white essential oil in w/o emulsion at 45 min; for ring deformation (characteristic) (805 cm^{-1}). (Colors are visible in the online version of the article; <http://dx.doi.org/10.3233/SPE-2011-0526>.)

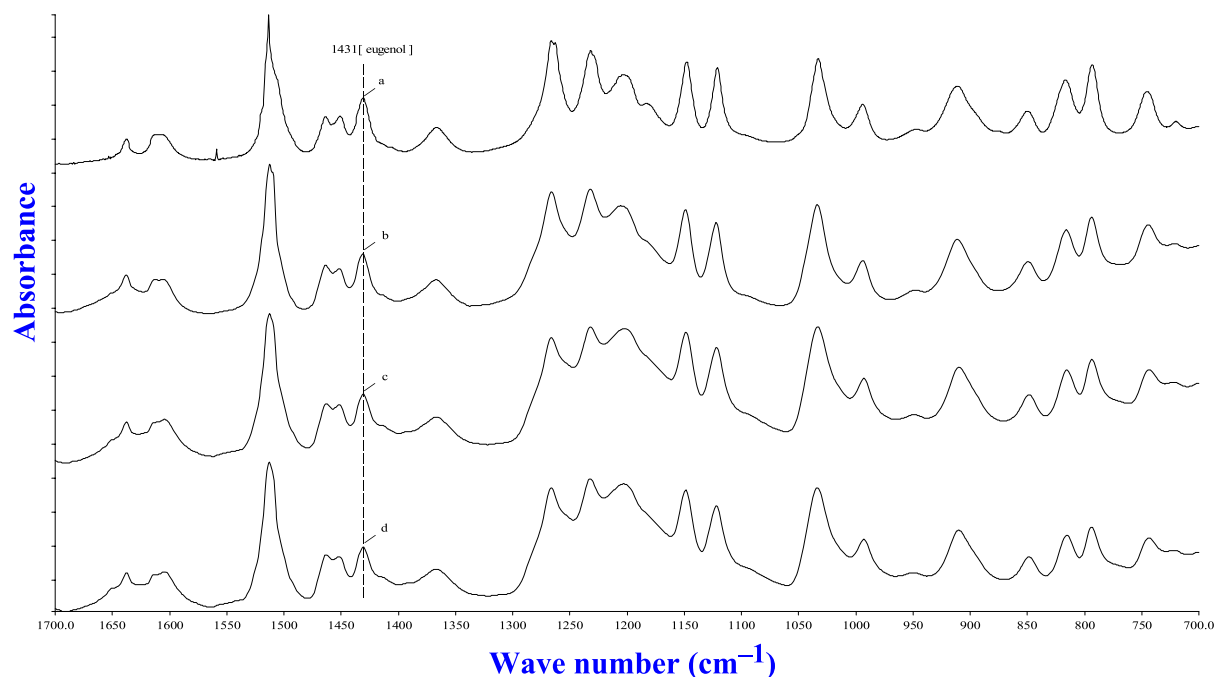


Fig. 6. ATR-IR spectra of human skin palm treated with (a) clove essential oil not in nano-emulsion; (b) clove essential oil in nano-emulsion at 0 min; (c) clove essential oil in nano-emulsion at 30 min; (d) clove essential oil in nano-emulsion at 60 min; for the CH₂ deformation vibration (characteristic) (1431 cm⁻¹). (Colors are visible in the online version of the article; <http://dx.doi.org/10.3233/SPE-2011-0526>.)

Table 2

Concentrations of eugenol, isoeugenol and methyl eugenol on human skin after treatment with various w/o, o/w and nano-emulsions by ATR-IR method

Sampling time (min)	Concentration on skin (mg/cm ²) ± SD ^a								
	Eugenol			Isoeugenol			Methyl eugenol		
	w/o	o/w	nano	w/o	o/w	nano	w/o	o/w	nano
0	18.5 ± 0.08	33.3 ± 0.24	41.9 ± 0.19	43.9 ± 2.2	47.1 ± 1.6	87.4 ± 1.7	30.2 ± 1.7	30.6 ± 1.3	25.4 ± 0.81
30	17.2 ± 0.37	32.5 ± 0.25	14.7 ± 0.01	27.2 ± 8.8	26.4 ± 1.2	38.5 ± 0.11	32.7 ± 3.3	26.4 ± 3.9	18.4 ± 0.54
60	15.4 ± 0.11	32.0 ± 0.48	10.4 ± 0.25	20.7 ± 1.4	17.2 ± 7.8	24.2 ± 15	29.3 ± 1.5	25.4 ± 5.7	16.3 ± 1.8

^aSD: Standard deviation.

appears to be an effective alternative for examining the absorption of eugenol derivatives into skin when compared with the traditional method of tape-stripping sampling followed by extraction and gas chromatography analysis.

Acknowledgement

This work was financially supported by grant NSC 96-2113-M-041-003-MY3 from the National Science Council, Taiwan.

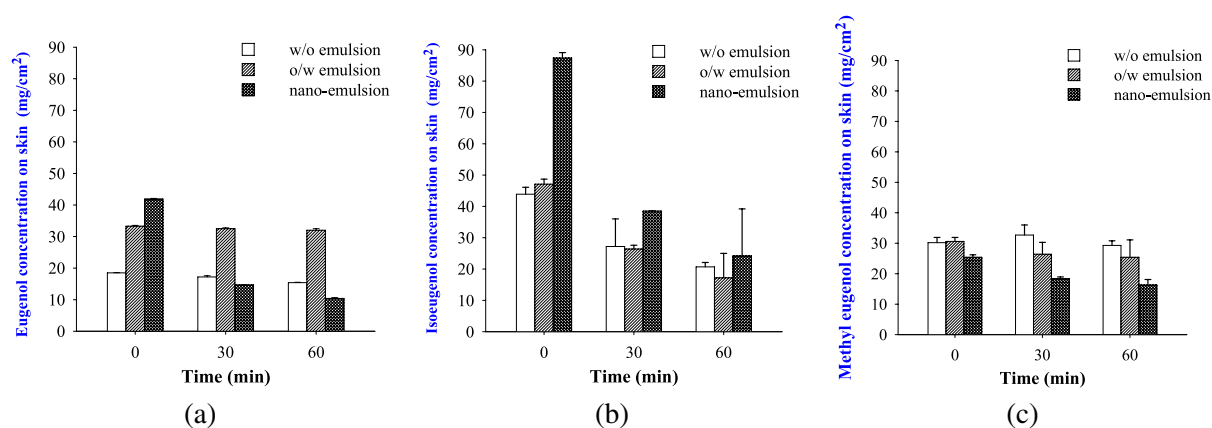


Fig. 7. Concentrations of (a) eugenol, (b) isoeugenol and (c) methyl eugenol on human skin after treatment with various w/o emulsion, o/w emulsion and nano-emulsion. Columns show mean concentrations; bars show standard deviation. (Colors are visible in the online version of the article; <http://dx.doi.org/10.3233/SPE-2011-0526>.)

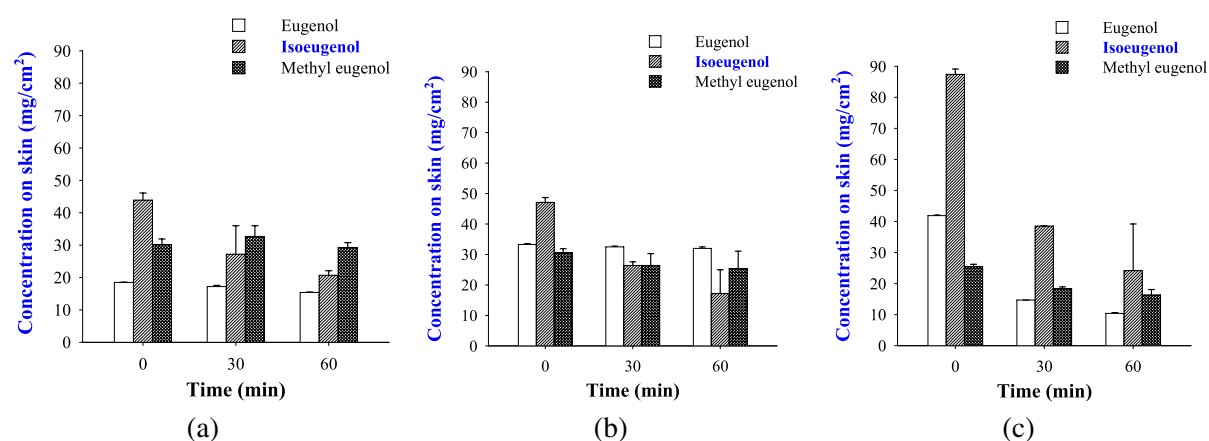


Fig. 8. Time course of the percutaneous absorption of eugenol, isoeugenol, and methyl eugenol after treatment with (a) w/o emulsion; (b) o/w emulsion; and (c) nano-emulsion of clove, cassia bark and thymes. (Colors are visible in the online version of the article; <http://dx.doi.org/10.3233/SPE-2011-0526>.)

References

- [1] T. Atsumi, S. Fujisawa and K. Tonosaki, A comparative study of the antioxidant/prooxidant activities of eugenol and isoeugenol with various concentrations and oxidation conditions, *Toxicol. In Vitro* **19** (2005), 1025–1033.
- [2] M. Baranska, H. Schulz, H. Krüger and R. Quilitzsch, Chemotaxonomy of aromatic plants of the genus *Origanum* via vibrational spectroscopy, *Anal. Bioanal. Chem.* **381** (2005), 1241–1247.
- [3] M. Baranska, H. Schulz, S. Reitzenstein, U. Uhlemann, M.A. Strehle, H. Krüger, R. Quilitzsch, W. Foley and J. Popp, Vibrational spectroscopic studies to acquire a quality control method of Eucalyptus essential oils, *Biopolymers* **78** (2005), 237–248.
- [4] M. Baranska, H. Schulz, A. Walter, P. Rösch, R. Quilitzsch, G. Lösing and J. Popp, Investigation of eucalyptus essential oil by using vibrational spectroscopy methods, *Vib. Spectrosc.* **42** (2006), 341–345.
- [5] C. Deng, S. Lin, T. Huang, G. Duan and X. Zhang, Development of gas chromatography/mass spectrometry following headspace solid-phase microextraction for fast determination of asarones in plasma, *Rapid Commun. Mass Spectrom.* **20** (2006), 2120–2126.
- [6] J. Fiori, M. Hudaib, L. Valgimigli, S. Gabbanini and V. Cavrini, Determination of *trans*-anethole in *Salvia sclarea* essential oil by liquid chromatography and GC–MS, *J. Sep. Sci.* **25** (2002), 703–709.

- [7] M. Ganzera, E.P. Ellmerer-Muller and H. Stuppner, Cycloartane triterpenes from *Combretum quadrangulare*, *Phytochemistry* **49** (1998), 835–838.
- [8] Y. Halim, S.J. Schwartz, D. Francis, N.A. Baldauf and L.E. Rodriguez-Saona, Direct determination of lycopene content in tomatoes (*Lycopersicon esculentum*) by attenuated total reflectance infrared spectroscopy and multivariate analysis, *J. AOAC Int.* **89** (2006), 1257–1262.
- [9] D.L. Heikes, SFE with GC and MS determination of safrole and related allylbenzenes in sassafras teas, *J. Chromatogr. Sci.* **32** (1994), 253–258.
- [10] N.A. Kocaoglu-Vurma, A. Eliardi, M.A. Drake, L.E. Rodriguez-Saona and W.J. Harper, Rapid profiling of Swiss cheese by attenuated total reflectance (ATR) infrared spectroscopy and descriptive sensory analysis, *J. Food Sci.* **74** (2009), S232–S239.
- [11] M. Križman, D. Baričević and M. Prošek, Fast quantitative determination of volatile constituents in fennel by headspace-gas chromatography, *Anal. Chim. Acta* **557** (2006), 267–271.
- [12] M. Mori, N. Ikeda, Y. Kato, M. Minamino and K. Watabe, Quality evaluation of essential oils, *Yakugaku Zasshi* **122** (2002), 253–261 (in Japanese).
- [13] L.E. Rodriguez-Saona, N. Koca, W.J. Harper and V.B. Alvarez, Rapid determination of Swiss cheese composition by Fourier transform infrared/attenuated total reflectance spectroscopy, *J. Dairy Sci.* **89** (2006), 1407–1412.
- [14] G.C. Santus and R.W. Baker, Transdermal enhancer patent literature, *J. Control. Release* **25** (1993), 1–20.
- [15] M. Sari, D.M. Biondi, M. Kaâbeche, G. Mandalari, M. D'Arrigo, G. Bisignano, A. Saija, C. Daquino and G. Ruberto, Chemical composition, antimicrobial and antioxidant activities of the essential oil of several populations of Algerian *Origanum glandulosum* Desf, *Flavour Fragr. J.* **21** (2006), 890–898.
- [16] H. Schulz and M. Baranska, Identification and quantification of valuable plant substances by IR and Raman spectroscopy, *Vib. Spectrosc.* **43** (2007), 13–25.
- [17] H. Schulz, M. Baranska, R. Quilitzsch, W. Schütze and G. Lösing, Characterization of pepper corn, pepper oil, and pepper oleoresin by vibrational spectroscopy methods, *J. Agr. Food Chem.* **53** (2005), 3358–3363.
- [18] H. Schulz, G. Özkan, M. Baranska, H. Krüger and M. Özcan, Characterisation of essential oil plants from Turkey by IR and Raman spectroscopy, *Vib. Spectrosc.* **39** (2005), 249–256.
- [19] A. Smelcerovic, M. Spiteller, A.P. Ligon, Z. Smelcerovic and N. Raabe, Essential oil composition of *Hypericum* L. species from Southeastern Serbia and their chemotaxonomy, *Biochem. Syst. Ecol.* **35** (2007), 99–113.
- [20] R.L. Smith, T.B. Adams, J. Doull, V.J. Feron, J.I. Goodman, L.J. Marnett, P.S. Portoghese, W.J. Waddell, B.M. Wagner, A.E. Rogers, J. Caldwell and I.G. Sipes, Safety assessment of allylalkoxybenzene derivatives used as flavouring substances – methyl eugenol and estragole, *Food Chem. Toxicol.* **40** (2002), 851–870.
- [21] J. Viyoch, N. Pisutthanan, A. Faikreua, K. Nupangta, K. Wangtorpol and J. Ngokkuen, Evaluation of *in vitro* antimicrobial activity of Thai basil oils and their micro-emulsion formulas against *Propionibacterium acnes*, *Int. J. Cosmet. Sci.* **28** (2006), 125–133.
- [22] L.H. Wang and J.X. Chen, Study of p-aminobenzoic acid and its metabolites in human volunteers treated with essential oil formulations using attenuated total reflection-Fourier transform infrared spectroscopy and HPLC with fluorometric detection, *Microchim. Acta* **168** (2010), 93–98.
- [23] L.H. Wang, H.J. Liu and I.M. Ling, Essential-oil creams as carriers for the percutaneous absorption of eugenol: evaluation *in vivo*, *Trends Chromatogr.* **5** (2009), 21–25.
- [24] L.H. Wang, C.C. Wang and S.K. Chuang, Simultaneous determination of alkenyl benzenes in essential oils and human serum by gas chromatography and GC–MS, *Asian J. Chem.* **22** (2010), 3835–3842.



Hindawi

Submit your manuscripts at
<http://www.hindawi.com>

